ChemPhysChem

Research Article
doi.org/10.1002/cphc.202200204

Chemistry Europe
European Chemical Societies Publishing

www.chemphyschem.org

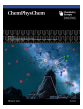

Use of 5,10-Disubstituted Dibenzoazaborines and Dibenzophosphaborines as Cyclic Supports of Frustrated Lewis Pairs for the Capture of CO_2

Maxime Ferrer,[a, b] Ibon Alkorta,*[a] Jose Elguero,[a] and Josep M. Oliva-Enrich[c]

The reactivity of 5,10-disubstituted dibenzoazaborines and dibenzophosphaborines towards carbon dioxide was studied at the DFT, M06-2X/def2-TZVP, computational level. The profile of this reaction comprises of three stationary points: the pre-reactive complex and adduct minima and the transition state(TS) linking both minima. Initial results show that dibenzoazaborines derivatives are less suitable to form adducts with CO_2 than dibenzophosphaborine systems. The influence of the basicity on the P atom and the acidity on the B center of the dibenzophosphaborine in the reaction with CO_2 was also explored. Thus, an equation was developed relating the properties (acidity, basicity and boron hybridization) of the isolated dibenzophosphaborine derivatives with the adduct energy. We found that modulation of the boron acidity allows to obtain more stable adducts than the pre-reactive complexes and isolated monomers.

Introduction

The concepts of acidity and basicity are of paramount importance in chemistry, with different definitions found in the literature. The Lewis acidity/basicity concept, defined by Lewis himself in 1923,[1] is possibly the most popular describing a Lewis acid (LA) as an electron-pair acceptor, and a Lewis base (LB) as an electron-pair donor. This definition enables the understanding of the direct formation of the $F_3B{:}NH_3$ Lewis adduct by the interaction between BF_3 (a Lewis acid) and NH_3 (a Lewis base). In this adduct, the N atom donates its pair of electrons to the B atom which is the electron acceptor.[2] The prevention of this contact or donation is known as Frustrated Lewis Pair (FLP), a concept introduced by Stephan *et al.* in 2006.[3] From an electronic structure point of view, preventing the contact between a LA and a LB creates a "frustration" in the system. The use of large substituents on the LA and LB units, and/or the modification of the molecule skeleton separates the acid and basic centers which partially blocks the electron-transfer between the base and the acid, thus enhancing their simultaneous reactivity toward a third molecule.

The use of FLP as metal-free catalysts is part of the "green chemistry" tendency. In the last decade, FLPs have been used to chemically activate a large set of small molecules,[4–6] considering that the electron density of the small molecule, generally known to be very stable, is disturbed by a bilateral attack of the FLP. This simultaneous attack facilitates the rupture of small molecules such as H_2 or the capture of small systems such as CO_2. In particular, the capture and sequestration of CO_2 is of great relevance for global warming as has been highlighted in recent reviews.[7–12] In fact, a combined search of the "frustrated Lewis pair" and "carbon dioxide" terms in the Web of science provides 400 results, 49 of which are review articles.

The ability of FLPs to capture CO_2 is known experimentally since 2009.[13,14] Nowadays, effective FLPs used to capture CO_2 expand from the typical N/B and P/B FLPs,[13–18] to some rhenium based,[19] bridged,[20] and cyclic FLP,[21] passing through more exotic ones containing germanium,[22] aluminum,[23,24] or copper,[25–28] and even including them in polymers.[29,30] In addition, FLPs are being used to activate CO_2 and reduce it to useful chemicals,[5,31–33] like for example methanol,[24,25,34] methane,[35] formates,[17,31] methoxysilane,[36] in a catalytic fashion or not. Theoretical studies were added to those experimental results, to better understand the reaction mechanism behind the capture and reduction of CO_2, as well as proposing a systematic way to improve the existing FLP playing with the intrinsic properties of the atoms involved.[18,22,37–51]

Considering phosphorus as a LB, boron as a LA, and that the distance between both atoms, may be imposed by a ring structure and/or large substituents, it is possible to design FLP systems to capture CO_2. Among potential intramolecular FLPs, the tricyclic derivatives of 9,10-dihydroanthracene (DHA) with different substituents in positions 9 and 10 should be mentioned (Figure 1).[52–58] The presence of the aromatic rings

[a] M. Ferrer, Prof. I. Alkorta, Prof. J. Elguero
Instituto de Química Médica (CSIC)
Juan de la Cierva, 3, 28006 Madrid, Spain
E-mail: ibon@iqm.csic.es
Homepage: http://are.iqm.csic.es
[b] M. Ferrer
PhD Program in Theoretical Chemistry and Computational Modeling,
Doctoral School, Universidad Autónoma de Madrid
28049 Madrid, Spain
[c] Dr. J. M. Oliva-Enrich
Instituto de Química-Física Rocasolano (CSIC)
Serrano, 119, 28006 Madrid, Spain

Supporting information for this article is available on the WWW under https://doi.org/10.1002/cphc.202200204

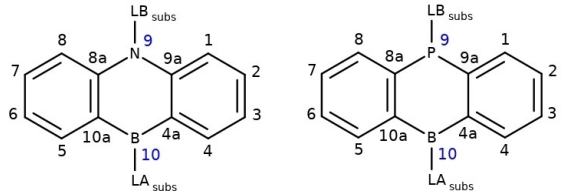

Figure 1. Scheme of the N/B and P/B ring systems 5,10-dihydrodibenzo[*b*,*e*][1,4]azaborine (left) and 5,10-dihydrodibenzo[*b*,*e*][1,4]phosphaborine (right) showing the corresponding numbering.

connecting the acid and basic center can enhance their properties as electron acceptor/donor, respectively. Searching the Cambridge Structural Database (CSD), twelve X-ray structures of DHA derivatives with N/B and P/B pairs in positions 9 and 10 linked to a variety of substituents (i.e from a H atom to large groups such as mesityl) were found.[53–58] From these, nine contain the N/B pair (Refcodes: COYNEK, FUTBAX, MUKLAI, QIXYUU, QIXZAB, QIXZEF, QIXZIJ, RERPEK, YAGKUM), whereas three contain the P/B pair (Refcodes: QAYDUQ, RERPOU, YIHBEX). In all structures, the pnictogen atom is linked to a H atom, a methyl group or an aromatic ring and the B atom is bonded to a substituted aromatic ring, hydroxyl groups, or Cl atoms. Analogous saturated six-membered rings with the phosphorous and boron groups in 1/4 positions has been shown to react as FLP vs. alkenes, alkynes and CO_2.[59]

In the present study, the corresponding stationary points (minima and TSs) for the reaction between DHA derivatives containing P/B and N/B pairs in positions 9/10 with a variety of substituents and CO_2 have been obtained utilizing quantum-chemical computations. Based on these studies, an equation has been developed linking the acid and basic properties of the isolated DHA derivatives to their ability to form CO_2 adducts.

Computational Details

Optimizations were carried out with the M06-2X DFT functional[60] and the def2-TZVP basis set[61] using the scientific software Gaussian16.[62] Frequency calculations of all optimized systems at the same level of theory confirm that they were minima (no imaginary frequencies) or TSs (one imaginary frequency).

The Natural Bond Orbital method[63] was applied on some compounds to explain the orbital interactions utilizing the NBO-7.0 program.[64] For example, the charge transfer stabilization energy between the bonding and anti-bonding orbitals of the π-system indicates the strength of the π-delocalization. All the NBO calculations were performed using the M06-2X/def2-TZVP level of theory.

The Molecular Electrostatic Potential (MEP) was computed on the 0.001 a.u. electron density isosurface with the Multiwfn[65] software, using the M06-2X/def2-TZVP wavefunction. The MEP corresponds to the interaction energy of a non-polarizing positive charge (+ 1.0 e) with the molecule on the 0.001 a.u. electron density isosurface. Analysis of MEP allows to localize nucleophilic molecular regions (minima of the MEP), or electrophilic ones (maxima of the MEP). For the systems studied in this work, a MEP minimum on the pnictogen atoms (P and N) and a maximum on the boron atom are expected for the DHA derivatives. Ideally, the MEP of the DHAs should be complementary to that of CO_2 which presents a MEP maximum around the carbon atom, and two MEP minima on the oxygen atoms.[66]

The topological properties of the systems' electron density were analyzed by means of the quantum theory of Atoms In Molecules (QTAIM)[67,68] model as implemented in the scientific software AIMAll.[69] The electron density critical points (CPs) were localized by the computation of the density gradient. Using the signature of the second derivative matrix (Laplacian), the CPs were classified as attractor, bond, ring or cage critical points; from a chemical point of view, the most interesting CPs are the Bond Critical Points (BCP). The Laplacian, the potential density energy and the kinetic density energy at these BCPs give information about the covalent character of the interaction.[70,71] The molecular graphs were also computed and plotted with the AIMAll software[69] at the M06-2X/def2-TZVP level of theory.

The complexes' binding energy (E_b) was calculated as the difference between the energy of the complex ($E_{complex}$) and the energy of the optimized monomers (E_{DHA} and E_{CO2}) (Equation 1). Similarly, the interaction energy (E_{int}) was obtained using the energy of the monomers with the geometry within the complex (E'_{DHA} and E'_{CO2}) (Equation 2). The difference between the binding energy and the interaction energy is the total deformation energy (E_{def}) (Equation 3). Both E_{int} and E_{def} parameters were used to analyze the complex formation as the monomers approach each other.[72–74]

$$E_b = E_{complex} - E_{DHA} - E_{CO_2} \quad (1)$$

$$E_{int} = E_{complex} - E'_{DHA} - E'_{CO_2} \quad (2)$$

$$E_{def} = (E_{DHA} - E\prime_{DHA}) + \left(E_{CO_2} - E\prime_{CO_2}\right) = E_b - E_{int} \quad (3)$$

The basicity and acidity of the isolated DHA derivatives was evaluated from its proton affinity (PA) and fluoride ion affinity (FIA),[75–77] respectively (Eqs. 4 and 5). The enthalpies (H) of the different compounds in Eqs. 4 and 5 are used to calculate the PAs and FIAs. Using the parameters defined by Eqs. (1–5), we are able to rationalize the reactivity of the DHAs derivatives with CO_2.

$$[LB-H]^+ \rightarrow LB + H^+;\ PA = H(LB) + H(H^+) - H([LB-H]^+) \quad (4)$$

$$[LA-F]^- \rightarrow LA + F^-;\ FIA = H(LA) + H(F^-) - H([LA-F]^-) \quad (5)$$

Results and Discussion

Isolated DHA Derivatives with N/B and P/B Pairs

A simplified nomenclature for the DHA derivatives (i.e. LB-LB_{subs}-LA-LA_{subs}) will be used from here on. As shown in Figure 2, LB stands for Lewis base (N or P), LA for Lewis acid (B) and LB_{subs} and LA_{subs} stand for the substituent on the LB and LA, respectively.

Four DHA derivatives were chosen (N-H-B-Cl, P-H-B-Cl, N-Ph-B-Cl, and P-Ph-B-Cl, Figure 2) based on those synthesized by Ishikawa *et al.*[56] (N-H-B-Cl, Figure 2) and Agou *et al.*[53] (P-Ph-B-Mes, Mes = Mesityl). Based on literature reports, when a FLP captures CO_2 the interaction is bilateral meaning that the FLP-base attacks the σ-hole of the C atom and the FLP-acid accepts electron density from one of the O atoms. In general, the strongest interaction corresponds to the attack of the FLP-base

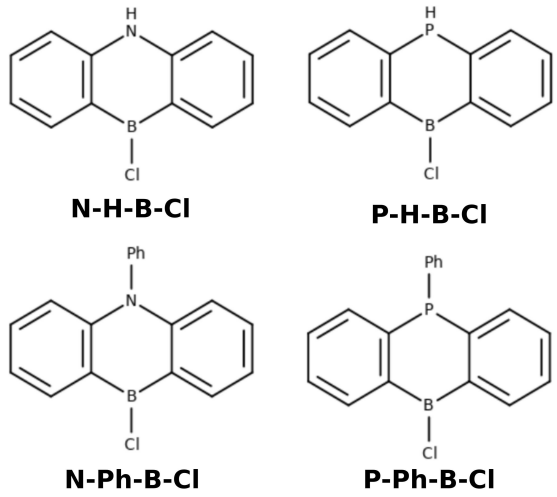

Figure 2. Structures of the DHA derivatives studied in this section indicating the nomenclature used.

to the C atom, what can be corroborated by the fact that some phosphines and N-heterocyclic carbenes (NHC)[78–80] are able to capture CO_2 without the need of an acid. In addition, nitrogen-containing compounds are experimentally used to capture CO_2 without the help of any Lewis acid.[81–83] For this reason, we focused our attention on the effect of the FLP-base (P or N) and its substituents (i.e. H or Ph). As regards to the FLP-acid center (B), we chose the smallest substituent found in the CSD for these systems (i.e. Cl) for computational considerations.

The optimized geometries of the four monomers studied (N-H-B-Cl, N-Ph-B-Cl, P-H-B-Cl, P-Ph-B-Cl) are shown in Figure 3. Significant differences are observed in the geometries of N and P derivatives; thus, the N-containing central ring of the tricyclic core is flat, while in the systems with P that ring is not planar.

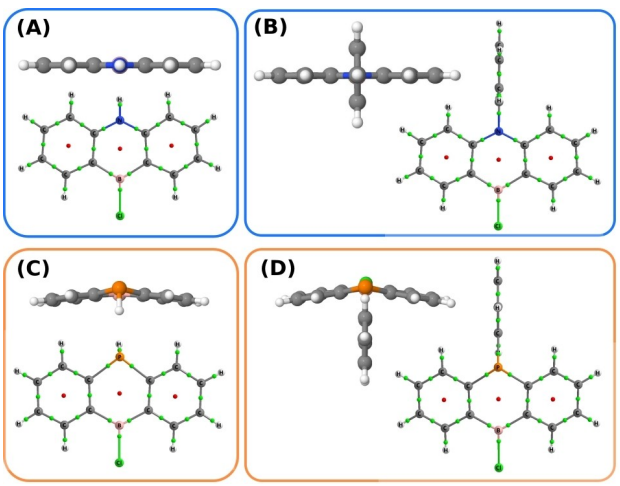

Figure 3. Optimized structures and QTAIM molecular graphs of the (A) N-H-B-Cl, (B) N-Ph-B-Cl, (C) P-H-B-Cl, and (D) P-Ph-B-Cl DHA derivatives. BCP and RCP are represented by green and red dots, respectively.

These differences can be explained based on the delocalization of the pnictogen lone pair. Thus, the lone pair on the N atom is delocalized into the lateral phenyl rings, while this delocalization is weaker in the case of P-containing DHA systems. This feature can be verified by NBO calculations. For instance, in the N-Ph-B-Cl system, the interaction between the natural lone pair of the N atom and the natural π-anti-bonding orbitals C(4a)-C(9a) and C(8a)-C(10a) amounts to 243 kJ·mol^{-1}. However, in the case of the P-Ph-B-Cl derivative, these interaction amounts to 36 kJ·mol^{-1}, almost seven times lower as compared to the N-Ph-B-Cl system.

Furthermore, the electron density at the BCP of the N–C bond in the N-[H/Ph]-B-Cl systems is close to that found for the pyridine [$BCP_{pyridine}$(N–C) = 0.35 a.u.; $BCP_{N\text{-}H\text{-}B\text{-}Cl}$(N–C) = 0.31 a.u.; $BCP_{N\text{-}Ph\text{-}B\text{-}Cl}$(N–C) = 0.30 a.u.], indicating the presence of an aromatic bond. It can be assumed that the delocalization of the N lone pair will limit the electron donation to the CO_2 carbon atom.

As mentioned, the MEP on the 0.001 a.u. electron density isosurface of the selected DHA derivatives were calculated and the results indicating the MEP maxima and minima associated to the LA and LB centers are shown in Figure 4. These maxima and minima (represented by singular points in Figure 4) vary in magnitude and position as a function of the different substituents and nature of the acidic/basic centers. Hence, in the N-H-B-Cl system, all the values observed are negative, being that of the maximum on the B atom of −6 kJ·mol^{-1} and that of

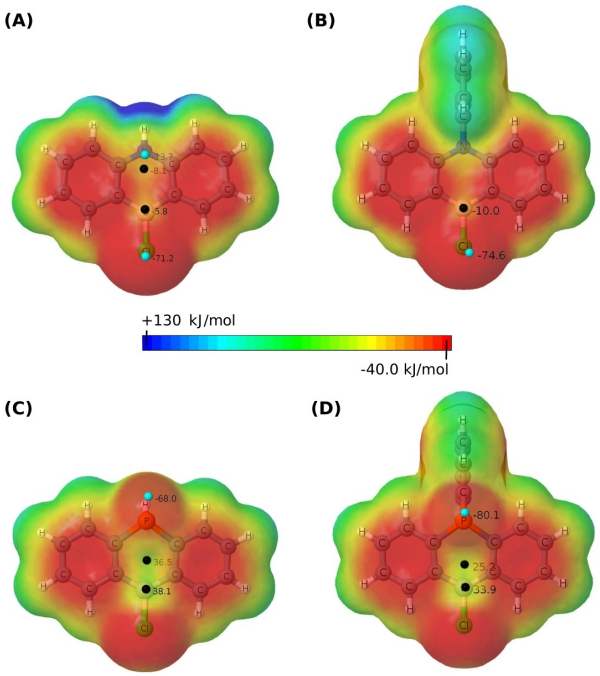

Figure 4. Molecular Electrostatic Potential (MEP) of the (A) N-H-B-Cl, (B) N-Ph-B-Cl, (C) P-H-B-Cl and (D) P-Ph-B-Cl DHA systems on the 0.001 a.u. electron density isosurface. A MEP range between −40 to 130 kJ·mol^{-1} was used for the plot. The positive regions are represented in blue and the negative ones in red. Only the most interesting MEP extrema were plotted and are indicated with dots (light blue for the minima and black for the maxima), and their values are given in kJ·mol^{-1}.

the minimum associated to the lone pair of the N, $-14\ kJ\cdot mol^{-1}$. Additionally, a maximum close to the middle of the central ring is found to have a value of $-8\ kJ\cdot mol^{-1}$. As it can be observed in Figure 4, substitution of H by a phenyl ring in N-H-B-Cl leads to the loss of the minimum associated to the N atom as well as the maximum found in the middle ring. However, a negative maximum of $-10\ kJ\cdot mol^{-1}$ on the B atom still is observed in the N-Ph-B-Cl system.

The P-H-B-Cl system presents a MEP minimum on the P atom, with a value of $-68\ kJ\cdot mol^{-1}$. Two maxima were also found in the B atom and the center of the ring with values of $+38$ and $+37\ kJ\cdot mol^{-1}$, respectively. In this case the substitution of a H atom by a phenyl ring increases the absolute value of the MEP minimum on the P atom, and it reduces the values of the positive maxima. It should be noticed that given the hybridization of P, the minimum on the pnictogen atom is not localized on top of it, as in the case of the B atom, but it points towards the outer part of the molecule. Additionally, substitution of the P atom with a phenyl ring reduces the distance between the MEP minimum and the maximum; indeed, in the case of the P-H-B-Cl system these are separated by 4.26 Å while in the case of P-Ph-B-Cl they are separated by only 3.62 Å.

Therefore, the main differences between the DHA systems with N and P are: (i) the sign of the B atom MEP maxima, implying in the case of the nitrogen systems a repulsive interaction between the boron and the oxygen, before the polarization plays its role, (ii) the absolute values of the MEP extrema, being larger, in absolute value, in the P-containing systems.

Reactivity of CO_2 with DHA Derivatives with N/B and P/B Pairs

In the calculated coordinate of the reaction between the selected DHA derivatives and CO_2 three stationary points were found, a minimum corresponding to a complex, another minimum corresponding to an adduct and a TS connecting them (Figure 5). Similar profiles have been described for other reactions with CO_2.[22,78–81,84]

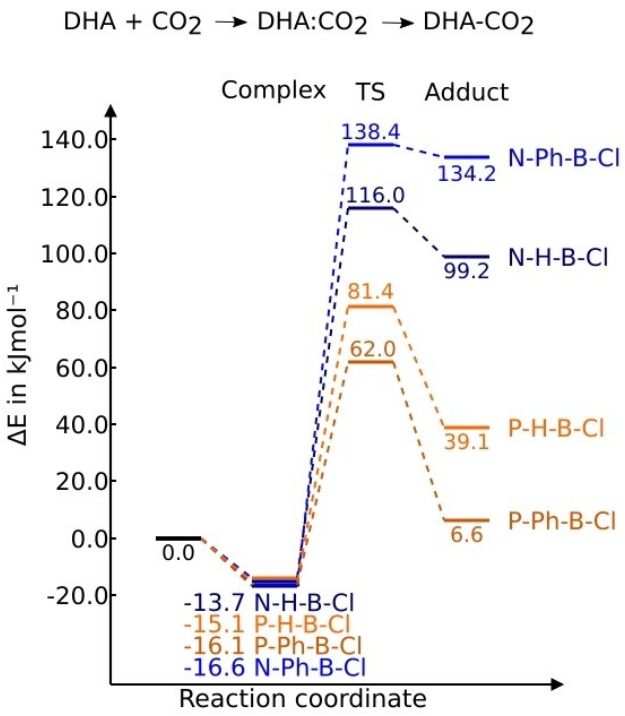

Figure 5. Reaction energy profiles for the reaction between compounds N-H-B-Cl, P-H-B-Cl, N-Ph-B-Cl, P-Ph-B-Cl and CO_2.

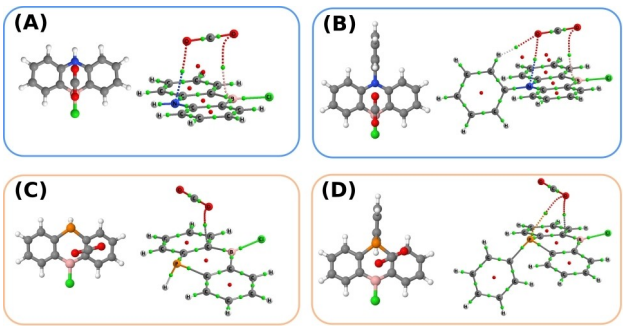

Figure 6. Optimized structures and QTAIM molecular graphs of the (A) N-H-B-Cl, (B) N-Ph-B-Cl, (C) P-H-B-Cl, and (D) P-Ph-B-Cl complexes with CO_2. BCP and RCP are represented by green and red dots, respectively.

From the Monomers to the Complexes

As shown in Figure 5, all complexes are more stable than the entrance channel, and very close in energy (around $-15\ kJ\cdot mol^{-1}$). The complexes formed with phenyl derivatives (i.e. N-Ph-B-Cl and P-Ph-B-Cl) are more stable than those unsubstituted in the pnicogen atoms (N-H-B-Cl and P-H-B-Cl) by $3\ kJ\cdot mol^{-1}$ and $1\ kJ\cdot mol^{-1}$, respectively. Even though these energy differences are rather small, the corresponding geometries are very different, as shown in Figure 6. In the case of complexes with the N systems, the CO_2 molecule is located on top of the central ring, thus enabling interactions between the O and N atoms with the B atoms. In the case of complexes formed by the P systems, the CO_2 molecule is tilted and located on top of one of the side rings.

A feature common to all the complexes formed by the charge transfer from the base lone pair towards the C–O antibonding orbitals is that the CO_2 molecule does not undergo any significant distortion. In fact, in the four systems the CO_2 molecule exhibits a C–O bond length around 1.16 Å, and a O–C–O angle around 179°, similar to the isolated system (i.e. 1.15 Å and 180°, respectively).

The positive sign of the MEP maxima on the B atom of the N-containing systems implies a repulsive interaction between the B and the O atoms of the CO_2 even before any polarization effect takes place (Figure 4). Therefore, it is interesting that even though the MEP values of P-containing monomers indicate a better disposition of these systems to interact with CO_2, the complexes formed show the weakest interactions.

Additionally, one of the major differences found in the MEPs of P- and N-systems was the positive maximum in the middle of the central ring in the P-derivatives (Figure 4); this prevents the positioning of the CO_2 molecule over the central ring, thus explaining the weak interactions.

The QTAIM molecular graphs of the four compounds are depicted in Figure 6. In the N-H-B-Cl:CO_2 complex, two bond paths are found between the DHA and the CO_2 molecule: one between one O and the N atom, and another between the other O and the B atom. In these two bond paths the corresponding BCP were found with electron density (ρ_{BCP}) values of 0.007 a.u. and 0.006 a.u., respectively. The presence of a phenyl substituent in the N atom of the DHA (N-Ph-B-Cl:CO_2) results in three intermolecular bond paths, the two previously mentioned plus an additional one between one of the O atoms and the H in *ortho* to the phenyl ring with a ρ_{BCP} of 0.006 a.u. This third BCP could explain the extra stabilization observed in the N-Ph-B-Cl:CO_2 *vs.* the N-H-B-Cl:CO_2 complexes.

As for the P-H-B-Cl:CO_2 complex, only one bond path is found between one of the CO_2 O atoms and the C(4a) atom of the naphthalene system with a ρ_{BCP} of 0.009 a.u. The introduction of a phenyl ring on the P atom results in an extra bond path between the same O atom and the P atom of the DHA with a ρ_{BCP} of 0.007 a.u.

From the Complexes to the Adducts

As mentioned before, the mechanism of the reactions studied involves the complexes discussed above to evolve towards the adducts through a TS (Figure 5). Several parameters of the calculated TSs and adducts are compiled in Figure 7 and Table 1.

With regards to the TS, the energy profiles of the reactions of P-containing DHA systems show lower energy barriers than those of the N-containing systems (Figure 5). The energy decomposition values indicate that the total energy of the TSs of the N-derivatives includes larger deformation energies, thus increasing the energy barrier (Table S6). This is directly related to the π-delocalization of the N atom penalizing the geometric deformation. It can also be pointed out that the introduction of a Ph ring destabilizes the N-containing TS but stabilizes the P-containing TS. This fact can be related to the hydrogen bond (HB) formation in the P-Ph-B-Cl:CO_2 TS, as opposed to the N-Ph-B-Cl:CO_2 TS, since in the latter this HB already existed in the original complex N-Ph-B-Cl:CO_2. QTAIM analysis showed that the ρ_{BCP} of the HB in the N-Ph-B-Cl:CO_2 TS increases by 0.012 a.u. compared to the ρ_{BCP} in the complex. The ρ_{BCP} at the HB in the P-Ph-B-Cl···CO_2 TS has a value of 0.010 a.u. Hence, the stabilization brought to the system by the formation of a HB in the TS is similar to that provided by forming the HB early in the complex.

Looking at the geometry of the TSs, major differences are observed upon Ph substitution in the pnictogen atoms. Contrary to the case of the complexes, where the introduction of a Ph substituent does not affect the DHA geometry, the changes observed between the unsubstituted and Ph substituted TSs are intrinsic to the TS, i.e. the substituents start to influence the system energy and geometry in the TS. Thus, in the TS of the N-substituted DHA derivatives, the introduction of a Ph ring induces a reduction of the N-C and B···O distances, the interaction energy increases by 41 kJ·mol^{-1} (in absolute value), and the DHA and CO_2 deformation energies increase respectively by 31 kJ·mol^{-1} and 33 kJ·mol^{-1}. Specifically, the increase in deformation energy is larger than the increase in interaction energy (64 kJ·mol^{-1} *vs.* 41 kJ·mol^{-1}) and therefore the activation barrier is larger. In the case of the P derivative TS, the introduction of a phenyl substituent decreases the P-C bond and elongates the B···O distance. This correlates with a strengthening of the P-C bond (as reflected in the increase of the ρ_{BCP} from 0.068 to 0.111 a.u.), causing a larger deformation in the geometry of the CO_2 molecule. However, the weakening of the B···O interaction reduces the deformation energy of the DHA, as the B atom remains in the plane of the central ring as reflected from the distance between the B atom and the plane defined by the central ring carbon atoms C(4a), C(8a), C(9a), and C(10a) (seen labels in Figure 1). Indeed, for the N-H-B-Cl and N-Ph-B-Cl systems, this B···O distance increases from 0.90 to 0.92 Å, respectively. In the P-H-B-Cl system this distance is 0.86 Å, and decreases to 0.81 Å for P-Ph-B-Cl.

Regarding the adducts, they present very similar geometries, and in particular the B···O distances are very analogous; thus, in the N-containing systems this distance is 1.58 Å and 1.55 Å for the P-containing ones. Similar to what was observed in the TSs, the N/B adducts are less stable than the P/B ones, and the introduction of a phenyl group had the same effect as in the TSs. However, now the energy difference between the CO_2 adducts with the N/B and P/B pairs is due to the interaction

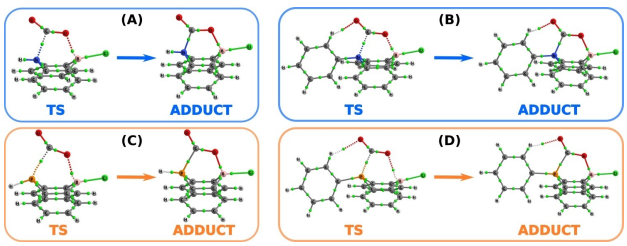

Figure 7. QTAIM molecular graphs of the TSs and Adducts of the systems (A) N-H-B-Cl, (B) N-Ph-B-Cl, (C) P-H-B-Cl, and (D) P-Ph-B-Cl.

Table 1. Distances of the P/N···C and B···O contacts in Å and the energy decomposition analysis (EDA) of the DHA–CO_2 interaction in kJ·mol^{-1}.

System	Interatomic distances		EDA		
	N/P···C	*B···O*	E_{int}	E_{def} *(DHA)*	E_{def} *(CO_2)*
N-H-B-Cl (TS)	1.94	1.81	−84.2	115.7	84.5
N-Ph-B-Cl (TS)	1.91	1.68	−125.4	146.9	117.1
P-H-B-Cl (TS)	2.32	1.89	−75.7	70.9	86.3
P-Ph-B-Cl (TS)	2.08	2.29	−116.0	49.0	129.2
N-H-B-Cl (add.)	1.59	1.58	−294.0	195.7	197.6
N-Ph-B-Cl (add.)	1.66	1.58	−269.9	199.7	204.5
P-H-B-Cl (add.)	1.89	1.55	−409.8	199.0	249.9
P-Ph-B-Cl (add.)	1.89	1.55	−442.5	188.8	260.3

energy between the two molecules and not to the deformation energy. Actually, the interaction energy in the adduct of the P/B system is about 1.5 times larger than that in the N/B systems (Table 1). This is related to the largest affinity of the P/B pair for the CO_2 molecule, because the P atom tends to be more hypercoordinating than the N atom.

Relationship Between the DHA Substituents and Adduct Stability

As mentioned in the previous section, the DHA derivatives with the N/B pair are not ideal for the capture of CO_2 due to the high TS energy barrier and low stability of the adducts. Accordingly, only the P/B systems will be further discussed.

Our study indicates that the reaction between the DHA derivatives and CO_2 proceeds in a one-step reaction from the pre-reactive complex because the contact between CO_2 and the acid and basic centers is simultaneous. These results agree with some previously described reactions involving preorganized P/B and P/Al FLPs[85,86] and contrast with other reactions described in the literature where no pre-reactive complex is formed[85] or the reaction proceeds in two steps.[86] In order to understand if these differences result from the P basicity and B acidity already mentioned in previous works,[52,87] we studied the effects of introducing different substituents in the DHA system. Thus, we analyzed the influence of the P basicity on the stability of the adduct, the effect of introducing a substituent in the B atom on the reaction profile, and the influence of the P basicity and B acidity on the adduct energy.

Phosphorus Basicity

The influence of the substitution on the P atom on the stability of the DHA CO_2 adducts was studied with no substituent (i.e. P-H-B-Cl) and with phenyl, methyl and *tert*-butyl substituents (i.e. P-Ph-B-Cl; P-CH_3-B-Cl, and P-*t*Bu-B-Cl). The relative stabilities obtained for the corresponding adducts and the proton affinities of the P atoms within the different DHAs are gathered in Table 2. Accordingly, the most basic system is P-*t*Bu-B-Cl with a PA of 987 $kJ\cdot mol^{-1}$, and the less basic is P-H-B-Cl with a PA of 928 $kJ\cdot mol^{-1}$. We observe that even though the basicity window of trisubstituted phosphines is wider than that in the DHAs here studied (233 $kJ\cdot mol^{-1}$ for the $P(R)_3$ series considered *vs.* 59 $kJ\cdot mol^{-1}$ in the DHAs, see Table 2), the ranking of basicity for the PR_3 series is analogous to that of the DHA series for similar substituents; thus, the calculated PA in DHA derivatives shows a linear relationship ($R^2=0.97$; Figure S1) with the experimental PA of the corresponding PR_3 . In addition, we found a second order polynomial correlation ($R^2=0.98$) between the stability of the DHA-CO_2 adducts and the PA of the isolated DHA. This correlation is also observed in the case of the P-R-B-F and P-R-B-Br series (Figure S2). Curiously, the *t*Bu substituted DHA is the most basic, but it does not lead to the most stable adduct.

Table 2. Adduct stability (with respect to the isolated monomers), computed proton affinity (PA) of the isolated DHA and experimental PA of the trisubstituted phosphines – NIST values.[18] All PA values are in $kJ\cdot mol^{-1}$.

R substituent in the P-R-B-Cl systems	Adduct Energy	PA	PA (PR_3) NIST
H	39.3	927.6	785.0
Ph	6.8	975.9	972.8
CH_3	1.6	968.4	958.8
*t*Bu	4.5	986.8	1017.9[*]

[*] Computed value with the G4 method.

Boron Acidity

Next, the reactivity of a series of DHA derivatives differently substituted on the B atom (F, Cl, Br, CH_3, CN, CF_3, NO_2, SiH_3, AlH_2 and OH) while maintaining the phenyl substituent on the P atom was studied. The relative energy of the adducts formed range from $+42$ to -35 $kJ\cdot mol^{-1}$ (Table 3). The calculated energy profiles of the reactions between DHAs with CF_3, NO_2 and CN as B-substituents and CO_2 show that the formation of the adduct is favored with respect to the isolated monomers (Figure 8). Depending on the substituent on the B atom we observe different scenarios. In the case of P-Ph-B-CN the calculated adduct is less stable than the complex; for the P-Ph-B-NO_2 DHA, we observe that the adduct obtained is slightly more stable than the complex; finally, in the case of the P-Ph-B-CF_3 DHA, the adduct with CO_2 is much more stable than the corresponding complex.

Considering that the activation energy of the reaction with P-Ph-B-CF_3 is around 50 $kJ\cdot mol^{-1}$ and that the corresponding adduct has a lower electronic energy than the complex, the preferred formation of the adduct was expected. In the case of the reactions with P-Ph-B-NO_2 and P-Ph-B-CN an equilibrium between complexes and adducts, limited by kinetic factors, is expected. As it can be observed in Figure 8, the corresponding adducts and complexes have similar energies; however, the activation energy is greater than 50 $kJ\cdot mol^{-1}$ in both cases. Therefore, since the CO_2 adduct with P-Ph-B-NO_2 is more stable, the equilibrium will be displaced toward the adduct, as it happened in the case of the P-Ph-B-CF_3 adduct. If the free

Table 3. Adduct stabilities ($kJ\cdot mol^{-1}$), fluorine affinities ($kJ\cdot mol^{-1}$), and boron *p/s* ratios of the isolated DHAs.

System	Adduct stability[a]	FIA	*p/s* ratio
P-Ph-B-F	18.9	368.5	3.04
P-Ph-B-Cl	6.8	392.0	2.65
P-Ph-B-Br	1.4	405.1	2.73
P-Ph-B-CH_3	2.7	351.4	1.92
P-Ph-B-CN	−10.2	417.4	2.70
P-Ph-B-CF_3	−34.6	428.4	2.52
P-Ph-B-NO_2	−20.9	444.1	3.02
P-Ph-B-SiH_3	7.8	382.5	1.99
P-Ph-B-AlH_2	−0.7	370.0	1.98
P-Ph-B-OH	42.1	327.8	2.43

[a] Calculated as the energy difference between the adduct and the isolated monomers (DHA + CO_2).

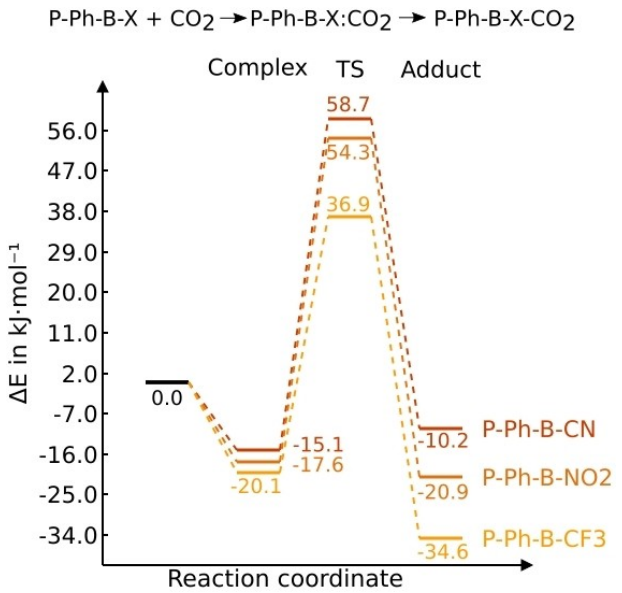

Figure 8. Reaction energy profiles for the reaction between compounds P-Ph-B-CN, P-Ph-B-NO_2, and P-Ph-B-CF_3 with CO_2 in vacuum.

energy is used instead of the electronic energy, a similar plot would be obtained (see the correlation between free and electronic energies in Figure S4) only with more positive values (by a factor around 58.0 kJ·mol^{-1}). Only a shift around 58.0 kJ·mol^{-1} toward positive values will be observed. Moreover, considering that in this reaction two species (one of them being a gas) are converted into one, the large entropy contribution will make the reaction non spontaneous.

We can hypothesize that the stability changes observed are related to the acidity of B, which is modulated by its substituents. Thus, in order to evaluate the acidity of the isolated DHAs, the fluoride ion affinity (FIA) was calculated (Table 3). The results obtained indicate that the most acidic B atom corresponds to the P-Ph-B-NO_2 compound (FIA = 444 kJ·mol^{-1}) while the less acidic is P-Ph-B-OH (328 kJ·mol^{-1}), being the obtained FIA range of 116 kJ·mol^{-1} approximately twice the range of the calculated P basicity (see Table 2). However, the correlation between the FIA and the adduct energy is not straightforward and more parameters are required. When comparing the N/B and P/B couples, we mentioned that the geometry of the monomers had an influence on the adducts energy. For that reason, we propose including as an independent variable the ratio between the *p* and *s* orbitals contribution (*p*/*s* ratio) in the B-LA_{subs} bond orbital as evaluated from the monomer NBO calculation.[87] The *p*/*s* ratio provides information about the hybridization of the B atom; for instance, a *p*/*s* ratio close to 3 indicates an sp^3 B atom. Considering that this parameter provides information about the geometry surrounding the atom, we can expect that a planar B atom with a vacant *p* orbital (i.e. with a *p*/*s* ratio close to 2) will be ideal for accepting electron density from one O atom of CO_2. Using the values listed in Table 3, the relative energy of the adducts can be correlated with the FIA and the *p*/*s* ratio (Equation 6).

$$Adduct\ Energy = (27.0 \pm 6.0) - (72.0 \pm 11.0)FIA + (23.0 \pm 9.0)p/s \quad (6)$$

$$n = 10 \quad R^2 = 0.87$$

According to Equation 6, the more acidic the B, the more stable the adduct. Therefore, if the B atom shows an sp^3 hybridization (*i.e.* *p*/*s* = 3) the formation of the adduct will be less favorable than with an sp^2 hybridized B. A similar equation using the *p*/*s* ratio, the van der Waals volume and the B charge was proposed by García-Lopez *et al.*[88] to predict the nucleophilicity of trivalent boron compounds.

Acidity/Basicity: Who is the Winner?

We have just discussed that for a given substituent on the B atom the stability of the adduct correlates with the P basicity by a second order polynomial, and for a given substituent on the P atom, the stability of the adduct correlates with the acidity of the B atom and the orbital contribution of the B–X bond.

Next, we try to assess the relative importance of the B acidity (i.e. FIA) and P basicity (i.e. PA) on the adduct stability using all the systems included in this work (i.e. the twelve already mentioned DHA systems plus P-H-B-F, P-H-B-Br, P-CH_3-B-F, and P-CH_3-B-Br). Thus, the ranges observed for each property and their average values are found to be different from one property to another. For comparative purposes, all parameters were normalized between 0.0 and 1.0 and they show average values between 0.5 and 0.7 (0.52 for FIA, 0.67 for PA, and 0.64 for the *p*/*s* ratio) and similar standard deviations (0.28 for FIA and PA, and 0.33 for the *p*/*s* ratio).

The resulting equation Equation (7) and the computed *vs.* fitted values plot are displayed in Figure 9, and a t-test was run to confirm that the statistical terms were significant (Table S5).

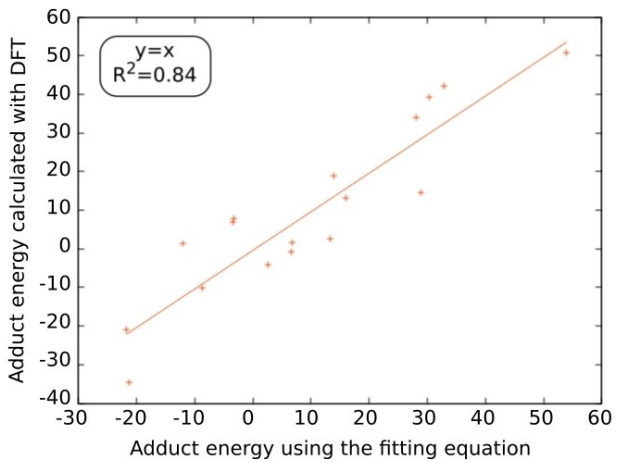

Figure 9. Fitted values of the adduct energy (kJ·mol^{-1}) using Equation 7 *vs.* those calculated at the M06-2X/def2-TZVP level of theory.

$$Adduct\ Energy = (99.0 \pm 15.0) - (87.0 \pm 11.0)\mathrm{FIA} - (68.0 \pm 12.0)\mathrm{PA} + (4.0 \pm 9.0)\mathrm{p/s} \quad (7)$$

$$n = 16,\ R^2 = 0.84$$

Following the results obtained with Equation 7 several conclusions may be reached. First, the main components controlling the stability of the adducts are the B acidity and the P basicity, being the former slightly more important than the latter in agreement with previous reports.[89] Second, the P basicity and B acidity are related, meaning that if the acidity of B increases, the basicity of P decreases and *vice versa*. In fact, removing the P-H-B-X compounds, a linear correlation with a negative slope can be found between the FIA and PA values, due to the delocalization of the P lone pair. Hence, when the B acidity increases, this atom is more able to accept electron density, thus pushing the P to share its lone pair with the π electrons in the central ring, thus decreasing its basicity. For example, by considering the monomers P-Ph-B-OH (FIA = 327.8 kJ·mol^{-1}), P-Ph-B-Cl (FIA = 392.0 kJ·mol^{-1}) and P-Ph-B-NO_2 (FIA = 444.1 kJ·mol^{-1}) and looking at the interactions between their P lone pair and the π system (from NBO calculations), we found that the larger the FIA, the larger the second order perturbation energy associated to those particular interactions [P-Ph-B-OH: 33.0 kJ·mol^{-1}; P-Ph-B-Cl: 35.7 kJ·mol^{-1}; P-Ph-B-NO_2: 36.5 kJ·mol^{-1}]. The inverse is also observed. Third, to understand why the P unsubstituted compounds do not follow this trend, we hypothesize that when the P lone pair is delocalized, a certain electron deficiency appears on the pnictogen atom. This deficiency can be compensated by the electronic effect of the P substituents, but in the case of the unsubstituted systems, this offset cannot be observed, or is very weak. Then, the unsubstituted P atom does not recover part of the electrons given to the π-system, thus lowering its basicity. This is the reason why, for a given FIA, the unsubstituted P compounds present a lower basicity than expected.

Finally, a correlation between the reaction energy barrier and the parameters of Equation 7 was found. The corresponding correlation coefficient is not too high ($R^2 = 0.79$), but it can be considered as acceptable (Table S6). Similar to what we observed for the adduct energy, the B acidity and P basicity are stabilizing the TS, but now, we found that the B acidity is more important. Also, the relevance of the B hybridization increases. Therefore, the stability of the adduct and TS can be described using the same statistical terms, but their relative importance is different.

Conclusions

The reactivity of substituted DHA towards carbon dioxide was studied using the M06-2X/def2-TZVP computational level, which includes dispersion corrections, and accordingly, the following conclusions can be reached. First, the P/B pair in position 9/10 of the DHA is the most suitable for capturing CO_2 as compared to the N/B pair. Second, B acidity and P basicity are the major components governing the stability of the final adduct, being the former slightly more relevant. Third, the acid and basic centers of the molecule are related; thus, an increase in B acidity reduces P basicity due to electron delocalization. Finally, it is possible to obtain adducts more stable than the complexes by modulating the B acidity, thus favorably tuning the CO_2 capture.

Acknowledgements

This work was carried out with financial support from the Ministerio de Ciencia, Innovación y Universidades (Projects PGC2018-094644-B-C2 and PID2021-125207NB-C32) and Dirección General de Investigación e Innovación de la Comunidad de Madrid (PS2018/EMT-4329 AIRTEC-CM). Thanks are given to the CTI (CSIC) and to the Irish Centre for High-End Computing (ICHEC, Dublin) for their continued computational support.

Conflict of Interest

The authors declare no conflict of interest.

Data Availability Statement

The data that support the findings of this study are available in the supplementary material of this article.

Keywords: boron hybridization · frustrated Lewis pairs · density functional calculations · dibenzoazaborines · carbon dioxide capture

[1] G. N. Lewis, *Trans. Faraday Soc.* **1923**, *19*, 452–458.
[2] A. C. Legon, H. E. Warner, *J. Chem. Soc. Chem. Commun.* **1991**, 1397–1399.
[3] G. C. Welch, R. R. San Juan, J. D. Masuda, D. W. Stephan, *Science* **2006**, *314*, 1124–1126.
[4] C. Jiang, O. Blacque, T. Fox, H. Berke, *Organometallics* **2011**, *30*, 2117–2124.
[5] F. G. Fontaine, D. W. Stephan, *Curr. Opin. Green Sustain. Chem.* **2017**, *3*, 28–32.
[6] A. E. Ashley, D. O'Hare, *Top. Curr. Chem.* **2012**, *334*, 191–217.
[7] N. Shreyash, M. Sonker, S. Bajpai, S. K. Tiwary, M. A. Khan, S. Raj, T. Sharma, S. Biswas, *Energies* **2021**, *14*, 4978.
[8] A. I. Osman, M. Hefny, M. I. A. Abdel Maksoud, A. M. Elgarahy, D. W. Rooney, *Environ. Chem. Lett.* **2021**, *19*, 797–849.
[9] I. Ghiat, T. Al-Ansari, *J. CO2 Util.* **2021**, *45*, 101432.
[10] S. Sun, H. Sun, P. T. Williams, C. Wu, *Sustain. Energy Fuels.* **2021**, *5*, 4546–4559.
[11] X. Wang, C. Song, *Front. Energy Res.* **2020**, *8*.
[12] A. Adamu, F. Russo-Abegão, K. Boodhoo, *BMC Chem. Eng.* **2020**, *2*, 2.
[13] C. M. Mömming, E. Otten, G. Kehr, R. Fröhlich, S. Grimme, D. W. Stephan, G. Erker, *Angew. Chem. Int. Ed.* **2009**, *48*, 6643–6646; *Angew. Chem.* **2009**, *121*, 6770–6773.
[14] D. W. Stephan, G. Erker, *Chem. Sci.* **2014**, *5*, 2625–2641.
[15] F. Bertini, V. Lyaskovskyy, B. J. J. a. Timmer, *J. Am. Chem. Soc.* **2012**, *134*, 201–204.
[16] Z. Lu, Y. Wang, J. Liu, Y. J. Lin, Z. H. Li, H. Wang, *Organometallics* **2013**, *32*, 6753–6758.

[17] I. Peuser, R. C. Neu, X. Zhao, M. Ulrich, B. Schirmer, J. A. Tannert, G. Kehr, R. Frhlich, S. Grimme, G. Erker, D. W. Stephan, *Chem. Eur. J.* **2011**, *17*, 9640–9650.
[18] J. J. Chi, T. C. Johnstone, D. Voicu, P. Mehlmann, F. Dielmann, E. Kumacheva, D. W. Stephan, *Chem. Sci.* **2017**, *8*, 3270–3275.
[19] Y. Jiang, O. Blacque, T. Fox, H. Berke, *J. Am. Chem. Soc.* **2013**, *135*, 7751–7760.
[20] B. Jiang, Q. Zhang, L. Dang, *Org. Chem. Front.* **2018**, *5*, 1905–1915.
[21] S. Dong, C. G. Daniliuc, G. Kehr, G. Erker, *Chem. Eur. J.* **2020**, *26*, 745–753.
[22] M. Ferrer, I. Alkorta, J. Elguero, J. M. Oliva-Enrich, *J. Phys. Chem. A.* **2021**, *125*, 6976–6984.
[23] C. Appelt, H. Westenberg, F. Bertini, A. W. Ehlers, J. C. Slootweg, K. Lammertsma, W. Uhl, *Angew. Chem. Int. Ed.* **2011**, *50*, 3925–3928; *Angew. Chem.* **2011**, *123*, 4011–4014.
[24] G. Ménard, D. W. Stephan, *J. Am. Chem. Soc.* **2010**, *132*, 1796–1797.
[25] C. M. Zall, J. C. Linehan, A. M. Appel, *ACS Catal.* **2015**, *5*, 5301–5305.
[26] C. M. Zall, J. C. Linehan, A. M. Appel, *J. Am. Chem. Soc.* **2016**, *138*, 9968–9977.
[27] R. Watari, S. Kuwata, Y. Kayaki, *Chem. Lett.* **2019**, *49*, 252–254.
[28] E. A. Romero, T. Zhao, R. Nakano, X. Hu, Y. Wu, R. Jazzar, G. Bertrand, *Nat. Catal.* **2018**, *1*, 743–747.
[29] L. Chen, R. Liu, Q. Yan, *Angew. Chem. Int. Ed.* **2018**, *57*, 9336–9340; *Angew. Chem.* **2018**, *130*, 9480–9484.
[30] T. A. R. Horton, M. Wang, M. P. Shaver, *Chem. Sci.* **2022**, *13*, 3845–3850.
[31] A. E. Ashley, D. O'Hare in *FLP-Mediated Activations and Reductions of CO2 and CO*, (Eds.: G. Erker, D. W. Stephan), Springer Berlin Heidelberg, Berlin, Heidelberg, **2013**, pp. 191–217.
[32] D. Ghosh, G. R. Kumar, S. Subramanian, K. Tanaka, *ChemSusChem* **2021**, *14*, 824–841.
[33] D. W. Stephan, *J. Am. Chem. Soc.* **2021**, *143*, 20002–20014.
[34] C. Das Neves Gomes, E. Blondiaux, P. Thuéry, T. Cantat, *Chem. Eur. J.* **2014**, *20*, 7098–7106.
[35] T. Wang, M. Xu, A. R. Jupp, Z.-W. Qu, S. Grimme, D. W. Stephan, T. Wang, M. Xu, A. R. Jupp, D. W. Stephan, T. Wang, Z. W. Qu, S. Grimme, *Angew. Chem. Int. Ed.* **2021**, *60*, 25771–25775.
[36] A. Berkefeld, W. E. Piers, M. Parvez, *J. Am. Chem. Soc.* **2010**, *132*, 10660–10661.
[37] S. Maeda, K. Ohno, *Chem. Phys. Lett.* **2004**, *398*, 240–244.
[38] Y. Kayaki, M. Yamamoto, T. Ikariya, *Angew. Chem. Int. Ed.* **2009**, *48*, 4194–4197; *Angew. Chem.* **2009**, *121*, 4258–4261.
[39] J. Baltrusaitis, E. V. Patterson, C. Hatch, *J. Phys. Chem. A* **2012**, *116*, 9331–9339.
[40] S. Wang, X. Wang, *Angew. Chem. Int. Ed.* **2016**, *55*, 2308–2320; *Angew. Chem.* **2016**, *128*, 2352–2364.
[41] A. P. de Lima Batista, A. G. S. de Oliveira-Filho, S. E. Galembeck, *ChemistrySelect* **2017**, *2*, 4648–4654.
[42] I. Alkorta, C. Trujillo, G. Sánchez-Sanz, J. Elguero, *Inorganics.* **2018**, *6*.
[43] G. Sánchez-Sanz, I. Alkorta, J. Elguero, C. Trujillo, *ChemPhysChem* **2019**, *20*, 3195–3200.
[44] D. Zhuang, A. M. Rouf, Y. Li, C. Dai, J. Zhu, *Chem. Asian J.* **2020**, *15*, 266–272.
[45] G. H. Gu, C. Choi, Y. Lee, A. B. Situmorang, J. Noh, Y.-H. Kim, Y. Jung, *Adv. Mater.* **2020**, *32*, 1907865.
[46] G. Sharma, P. D. Newman, J. A. Platts, *J. Mol. Graphics Modell.* **2021**, *105*, 107846.
[47] P. N. Nelson, *J. Mol. Struct.* **2021**, *1223*, 129212.
[48] S. Soroudi, M. Z. Kassaee, *J. Phys. Org. Chem.* **2022**, *35*, e4323.
[49] R. Pal, M. Ghara, P. K. Chattaraj, *Catalysts.* **2022**, *12*, 201.
[50] F. Buß, P. Mehlmann, C. Mück-Lichtenfeld, K. Bergander, F. Dielmann, *J. Am. Chem. Soc.* **2016**, *138*, 1840–1843.
[51] M.-A. Courtemanche, M.-A. Légaré, L. Maron, F.-G. Fontaine, *J. Am. Chem. Soc.* **2014**, *136*, 10708–10717.
[52] I. Cortés, J. J. Cabrera-Trujillo, I. Fernández, *ACS Org. Inorg. Au* **2021**, *2*, 44–52.
[53] T. Agou, J. Kobayashi, T. Kawashima, *Org. Lett.* **2005**, *7*, 4373–4376.
[54] T. Agou, J. Kobayashi, T. Kawashima, *Inorg. Chem.* **2006**, *45*, 9137–9144.
[55] T. Agou, J. Kobayashi, Y. Kim, F. P. Gabbaï, T. Kawashima, *Chem. Lett.* **2007**, *36*, 976–977.
[56] Y. Ishikawa, K. Suzuki, K. Hayashi, S. Y. Nema, M. Yamashita, *Org. Lett.* **2019**, *21*, 1722–1725.
[57] M. Kranz, F. Hampel, T. Clark, *J. Chem. Soc. Chem. Commun.* **1992**, *0*, 1247–1248.
[58] T. Agou, M. Sekine, J. Kobayashi, T. Kawashima, *J. Organomet. Chem.* **2009**, *694*, 3833–3836.
[59] X. Jie, Q. Sun, C. G. Daniliuc, R. Knitsch, M. R. Hansen, H. Eckert, G. Kehr, G. Erker, *Chem. Eur. J.* **2020**, *26*, 1269–1273.
[60] Y. Zhao, D. G. Truhlar, *Theor. Chem. Acc.* **2008**, *120*, 215–241.
[61] F. Weigend, R. Ahlrichs, *Phys. Chem. Chem. Phys.* **2005**, *7*, 3297–3305.
[62] M. J. Frisch, G. W. Trucks, H. B. Schlegel, G. E. Scuseria, M. A. Robb, J. R. Cheeseman, G. Scalmani, V. Barone, G. A. Petersson, H. Nakatsuji, X. Li, M. Caricato, A. V. Marenich, J. Bloino, B. G. Janesko, R. Gomperts, B. Mennucci, H. P. Hratchian, J. V. Ortiz, A. F. Izmaylov, J. L. Sonnenberg, Williams, F. Ding, F. Lipparini, F. Egidi, J. Goings, B. Peng, A. Petrone, T. Henderson, D. Ranasinghe, V. G. Zakrzewski, J. Gao, N. Rega, G. Zheng, W. Liang, M. Hada, M. Ehara, K. Toyota, R. Fukuda, J. Hasegawa, M. Ishida, T. Nakajima, Y. Honda, O. Kitao, H. Nakai, T. Vreven, K. Throssell, J. A. Montgomery Jr., J. E. Peralta, F. Ogliaro, M. J. Bearpark, J. J. Heyd, E. N. Brothers, K. N. Kudin, V. N. Staroverov, T. A. Keith, R. Kobayashi, J. Normand, K. Raghavachari, A. P. Rendell, J. C. Burant, S. S. Iyengar, J. Tomasi, M. Cossi, J. M. Millam, M. Klene, C. Adamo, R. Cammi, J. W. Ochterski, R. L. Martin, K. Morokuma, O. Farkas, J. B. Foresman, D. J. Fox in *Gaussian 16 Rev. A.03*, Wallingford CT, **2016**.
[63] F. Weinhold, C. R. Landis, *Valency and Bonding: A Natural Bond Orbital Donor-Acceptor Perspective*, Cambridge University Press, Cambridge, **2005**.
[64] E. D. Glendening, C. R. Landis, F. Weinhold, *J. Comput. Chem.* **2019**, *40*, 2234–2241.
[65] T. Lu, F. Chen, *J. Comput. Chem.* **2012**, *33*, 580–592.
[66] P. Raveendran, Y. Ikushima, S. L. Wallen, *Acc. Chem. Res.* **2005**, *38*, 478–485.
[67] R. F. W. Bader, *Atoms in Molecules. A Quantum Theory*, Clarendon, Oxford, U. K. **1990**.
[68] P. L. A. Popelier, *Atoms in Molecules. An Introduction*, Prentice-Hall, Manchester, U. K. **2000**.
[69] T. A. Keith, *AIMAll (Version 11.12.19)*; TK Gristmill Software, Overland Park KS; aim.tkgristmill.com.
[70] I. Mata, E. Molins, I. Alkorta, E. Espinosa, *J. Chem. Phys.* **2009**, *130*, 044104.
[71] I. Rozas, I. Alkorta, J. Elguero, *J. Am. Chem. Soc.* **2000**, *122*, 11154–11161.
[72] M. M. Montero-Campillo, I. Alkorta, J. Elguero, *Phys. Chem. Chem. Phys.* **2018**, *20*, 19552–19559.
[73] I. Alkorta, M. M. Montero-Campillo, J. Elguero, *Chem. Eur. J.* **2017**, *23*, 10604–10609.
[74] D. H. Ess, K. N. Houk, *J. Am. Chem. Soc.* **2007**, *129*, 10646–10647.
[75] P. Erdmann, J. Leitner, J. Schwarz, L. Greb, *ChemPhysChem.* **2020**, *21*, 987–994.
[76] I. B. Sivaev, V. I. Bregadze, *Coord. Chem. Rev.* **2014**, *270–271*, 75–88.
[77] A. K. Chandra, A. Goursot, *J. Phys. Chem.* **1996**, *100*, 11596–11599.
[78] C. T. Dewberry, R. D. Cornelius, R. B. Mackenzie, C. J. Smith, M. A. Dvorak, K. R. Leopold, *J. Mol. Spectrosc.* **2016**, *328*, 67–72.
[79] P. Mehlmann, C. Mück-Lichtenfeld, T. T. Tan, F. Dielmann, *Chem. Eur. J.* **2017**, *23*, 5929–5933.
[80] M. Prakash, K. Mathivon, D. M. Benoit, G. Chambaud, M. Hochlaf, *Phys. Chem. Chem. Phys.* **2014**, *16*, 12503–12509.
[81] T. S. Nguyen, C. T. Yavuz, *Chem. Commun.* **2020**, *56*, 4273–4275.
[82] B. Zhu, K. Li, J. Liu, H. Liu, C. Sun, C. E. Snape, Z. Guo, *J. Mater. Chem. A.* **2014**, *2*, 5481–5489.
[83] C. Petit, Y. Park, K.-Y. A. Lin, A.-H. A. Park, *J. Phys. Chem. C.* **2012**, *116*, 516–525.
[84] F. Bertini, F. Hoffmann, C. Appelt, W. Uhl, A. W. Ehlers, J. C. Slootweg, K. Lammertsma, *Organometallics* **2013**, *32*, 6764–6769.
[85] F. Bertini, F. Hoffmann, C. Appelt, W. Uhl, A. W. Ehlers, J. C. Slootweg, K. Lammertsma, *Organometallics.* **2013**, *32*, 6764–6769.
[86] F. Bertini, V. Lyaskovskyy, B. J. Timmer, F. J. De Kanter, M. Lutz, A. W. Ehlers, J. C. Slootweg, K. Lammertsma, *J. Am. Chem. Soc.* **2012**, *134*, 201–204.
[87] L. Liu, B. Lukose, B. Ensing, *ACS Catal.* **2018**, *8*, 3376–3381.
[88] D. W. Stephan, *J. Am. Chem. Soc.* **2015**, *137*, 10018–10032.
[89] D. García-López, J. Cid, R. Marqués, E. Fernández, J. J. Carbó, *Chem. Eur. J.* **2017**, *23*, 5066–5075.

Manuscript received: March 28, 2022
Revised manuscript received: June 14, 2022
Accepted manuscript online: June 15, 2022
Version of record online: July 14, 2022